

Josephson effect in cuprate superconducting structures

G. A. Ovsyannikov and K. Y. Constantinian

Citation: *Low Temp. Phys.* **38**, 333 (2012); doi: 10.1063/1.3702585

View online: <http://dx.doi.org/10.1063/1.3702585>

View Table of Contents: <http://ltp.aip.org/resource/1/LTPHEG/v38/i4>

Published by the [American Institute of Physics](#).

Related Articles

Spin-dependent transport properties through gapless graphene-based ferromagnet and gapped graphene-based superconductor junction

J. Appl. Phys. **112**, 013901 (2012)

Magnetoresistance in graphene-based ferromagnetic/ferromagnetic barrier/superconductor junction

J. Appl. Phys. **111**, 123908 (2012)

Josephson comparator with modified dynamic behavior for improved sensitivity

J. Appl. Phys. **111**, 123901 (2012)

Effect of thermal inhomogeneity for terahertz radiation from intrinsic Josephson junction stacks of $\text{Bi}_2\text{Sr}_2\text{CaCu}_2\text{O}_{8+\delta}$

Appl. Phys. Lett. **100**, 242603 (2012)

Two-dimensional magnetic field dependence of Josephson current and resonant current steps at finite voltage of square shape superconducting tunnel junctions

J. Appl. Phys. **111**, 113907 (2012)

Additional information on *Low Temp. Phys.*

Journal Homepage: <http://ltp.aip.org/>

Journal Information: http://ltp.aip.org/about/about_the_journal

Top downloads: http://ltp.aip.org/features/most_downloaded

Information for Authors: <http://ltp.aip.org/authors>

ADVERTISEMENT

**AIP**Advances

Submit Now

**Explore AIP's new
open-access journal**

- **Article-level metrics
now available**
- **Join the conversation!
Rate & comment on articles**

Josephson effect in cuprate superconducting structures

G. A. Ovsyannikov^{a)} and K. Y. Constantinian

Kotel'nikov Institute of Radio Engineering and Electronics of RAS, Mokhovaya 11-7, Moscow 125009, Russia
(Submitted October 13, 2011)

Fiz. Nizk. Temp. **38**, 423–433 (April 2012)

Electron transport and microwave properties of cuprate superconducting structures (bicrystal junctions and hybrid mesa heterostructures) are discussed here. Superconducting current in junctions from cuprate superconductors with the dominant $d_{x^2-y^2}$ -wave symmetry is determined by the barrier properties, characterized by the mid-gap bound states due to the multiple Andreev reflection. In bicrystal junctions it is revealed via linear dependence of critical current density on square root of the transparency, and an increase of spectral density of shot noise at low voltages are observed. The experiments demonstrate that the superconducting hybrid mesa-heterostructures have the critical current density $j_c = 1\text{--}700\text{ A/cm}^2$ for an antiferromagnetic interlayer with thickness $d_M = 10\text{--}50\text{ nm}$ and the characteristic decay length of superconducting correlations on the order of 7 nm, due to the anomalous long range proximity effect, analyzed in the model of coupled superconductors via multilayer magnetic layer with antiferromagnetic ordering of magnetization in the layers. It is found that the hybrid mesa-heterostructures have much greater sensitivity to external magnetic field than conventional Josephson junctions because of the strong dependence of superconducting current on interlayer spin state. © 2012 American Institute of Physics. [<http://dx.doi.org/10.1063/1.3702585>]

I. INTRODUCTION

Results of experimental studies of the Josephson Effect in cuprate-based thin film structures are discussed. Special attention was focused on the characteristics of the superconducting and quasiparticle current in Josephson junctions (JJ) caused by the presence of $d_{x^2-y^2}$ -type symmetry of the superconducting wave function in the superconductors (D-superconductors).

The influence of the Andreev states on the current-phase and temperature dependences of the superconducting current in bicrystal junctions in cuprate superconductors (CS) was experimentally investigated in Refs. 1–4. In Ref. 2 special features were observed in the current-voltage characteristics (CVC), which were caused by the low-energy Andreev levels. Low-energy Andreev states are manifested in bicrystal junctions of CS – both in electrophysical characteristics^{3,4} and in the appearance of excess shot noise at low voltages.^{5–8} Note that noise measurements give additional information about the conduction mechanism in the JJ.

Multilayer hybrid superconducting structures with alternating layers of ferromagnetics (F), normal metals (N), and insulators (I) have recently been of increased interest.^{9–12} The ability to manage the flow of current in such structures arises from the rotation of the magnetization direction in the F-layers under the influence of the magnetic field. Similar processes may occur in the antiferromagnetic (AF) layer that can be considered to be a collection of ferromagnetic layers of atomic thickness with oppositely directed magnetizations.^{13,14}

II. ANDREEV STATES AND THE JOSEPHSON EFFECT IN SUPERCONDUCTING BICRYSTAL JUNCTIONS FROM CUPRATE SUPERCONDUCTORS

Immediately after the discovery of the Josephson Effect it was noted^{15–17} that the transfer of the Cooper pairs through the potential barrier between two superconductors in the JJ

is due to the coherent Andreev reflection process. The order parameter in the CS has $d_{x^2-y^2}$ -type wave symmetry, i.e. in the ab -plane it changes the sign at a 90° change in direction of the quasiparticle momentum (see the inset in Fig. 1). As a result, in the junctions consisting of two misoriented by an angle α in the ab -plane D-superconductors the phase of the incident quasiparticles, which are also Andreev-reflected off the border, can have the opposite sign. The sequence of normal (mirror) and Andreev reflections in the (110) plane of the D-superconductor causes a number of related Andreev states with energies near the Fermi surface E_{MGS} ,^{18–20}

$$E_{MGS} = \pm \Delta_{R(L)}(\theta) \sin(\varphi/2) \sqrt{D(0)}, \quad (1)$$

where $\Delta_{R(L)}(\theta) = \Delta_0 \cos 2\theta$. In contrast to the SIS-tunneling transition (where S is a superconductor with the regular s -type symmetry of the order parameter) E_{MGS} levels even with small border transparency ($D \ll 1$) are located near the Fermi level, and their amplitude does not exceed $\Delta(\pi/4) \sqrt{D(\pi/4)}$.

The maximum energy values of the Andreev states at $\varphi = \pi$ depending on the angle of incidence θ at different angles α for a symmetrical JJ with a typical value of $D = 10^{-2}$ are shown in Fig. 2. For symmetrical JJs with $\alpha = 45^\circ$ low-energy Andreev states are observed for all the incident quasiparticles. With decreasing $\alpha < 45^\circ$ the range of angles θ , in which the E_{MGS} states are observed, equals 2α near the directions $\theta = \pm\pi/4$. Along the other directions states with energies close to the E_{SC} gap arise. For $\alpha = 0$ the situation is similar to the case of an SIS-junction, in which the Andreev states are described by the formula,

$$E_{SC} = \pm \Delta \sqrt{[(1 - D \sin^2(\varphi/2))]} \quad (2)$$

Since the superconducting current is determined by the energy of the Andreev states $I_S \propto dE_{MGS}/d\varphi$, with intermediate values

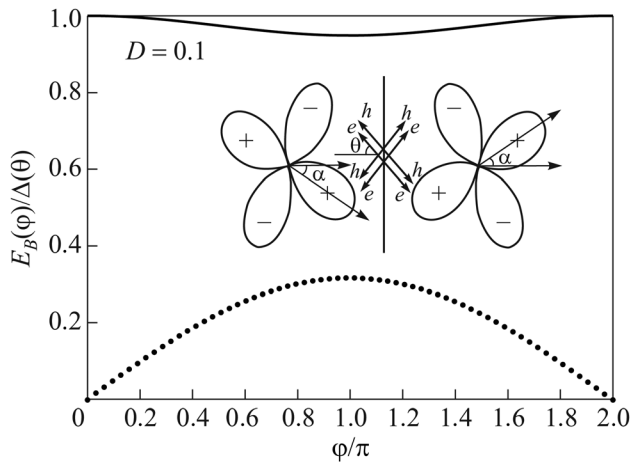


FIG. 1. Phase dependence of the Andreev levels in the tunnel junctions of S-superconductors (solid line) and low-energy Andreev levels of D-superconductors (dotted line) in the transparency of the boundary $D=0.1$. The inset shows a diagram of the bicrystal junction of two D-superconductors with a symmetrical misorientation of axes and the direction of incidence of electrons and holes.

$0 < \alpha < 45^\circ$ both contributions (1) and (2) should be taken into account by addition of currents.^{21–23} Note that for states (2) the current is proportional to the first degree, while in case (1)—to the quadratic root of the transparency of the boundary D . The tunneling cone (angular range) that determines the quasiparticles, which provide the main contribution to the current value, can be large $D(\theta) = D_0 (\cos \theta)^2$ for δ -like barriers and fairly narrow $\exp(2\theta)$ for wide barriers.²⁴

A. Experimental method

In the manufacturing of bicrystal JJs special characteristics of CS were used, manifesting in the fact that direct contact of two monocrystals of CS leads to a decrease of the critical current (the formation of weak coupling) in the junction, and the critical current value is strongly dependent on the angle of grain misorientation.²⁵ The most widely used are the “rotary” bicrystal junctions (RBJ), in which the weak coupling is formed by epitaxial misorientation around the c -direction of the CS. In the tilted bicrystal junctions (TBJ) there is a tilt in the basal planes of the CS around one of the

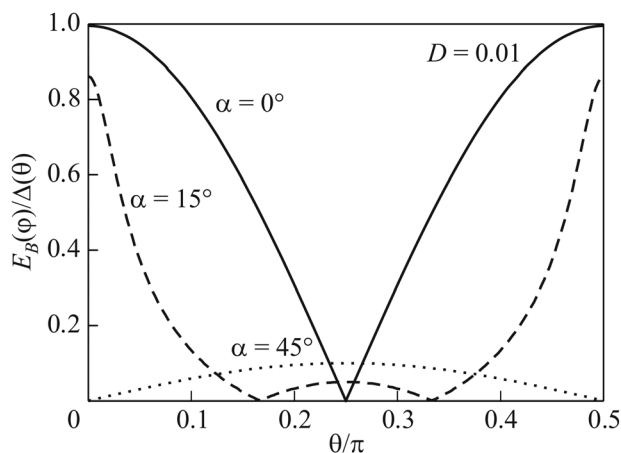


FIG. 2. The dependence of energies of the Andreev levels on the angle of incidence θ of quasiparticles with phase difference $\varphi = \pi$ for three values of angle α , which is the angle of misorientation of bicrystal rotational junctions of D-superconductors

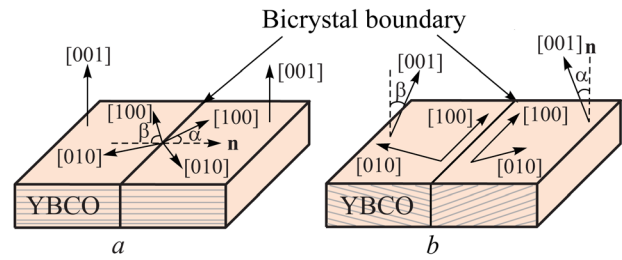


FIG. 3. Schematic representation of two types of bicrystal junctions: rotational (a) and tilted (b). The solid line indicates the bicrystal boundary, dotted line – the normal to the boundary or the plane of the substrate, shading is used to show the direction of the layers in cuprate superconductors.

directions, e.g. the a -axis (see Fig. 3). Misorientation of the crystallographic axes of the left and right parts of the junction to angles α and β to the normal to the plane of the interface (RBJ) or the substrate plane (TBJ) defines the electrophysical parameters of the JJ.^{26,27} In TBJ, as opposed to RBJ, the bicrystal boundary faceting is weaker.²⁶

Josephson junctions were fabricated on bicrystal substrates of NdGaO_3 (NGO) or sapphire. The (110) plane of NGO was selected as a reference, in which growth of the CS (001) $\text{YBa}_2\text{Cu}_3\text{O}_{7-\delta}$ (YBCO) film takes place, and the epitaxy condition $[100] \text{YBCO} // [001] \text{NGO}$ is satisfied, which persists at low tilt of the (110) NGO plane relative to the normal to the substrate.²⁸ Epitaxial YBCO films were deposited on the substrate surface by cathode sputtering in diode configuration in a dc discharge at high oxygen pressure or laser ablation. Spraying was carried out at $700\text{--}800^\circ\text{C}$. Bridges forming a transition $4 \mu\text{m}$ wide and $10 \mu\text{m}$ long, crossing the bicrystal junction, formed in the films either by ion-plasma or ion-beam etching.²⁹

Josephson junctions were obtained having critical current density $j_c = 10^4\text{--}10^5 \text{ A/cm}^2$ and characteristic voltage $V_c = I_c R_N = 1\text{--}2 \text{ mV}$ (where I_c is the critical current, and R_N is the resistance in the normal state) at $T = 4.2 \text{ K}$. Current-voltage characteristics (CVCs) were measured in the temperature range $4.2 \text{ K} < T < 77 \text{ K}$, in magnetic fields up to $H \leq 100 \text{ Oe}$, and under the influence of monochromatic microwave radiation at frequencies $f_e = 36\text{--}120 \text{ GHz}$. To carry out noise measurements a cooled HEMT transistor-based amplifier was used.³⁰ To reduce the influence of external electromagnetic fields the screening of microwave signals and filtering on all wires connected to the sample was utilized. Averaged over the directions of momentum, the transparency of barrier D was estimated from the value of characteristic resistance of the border with area S : $R_N S = (1\text{--}3) \cdot 10^{-7} \Omega\text{-cm}^2$ for RBJ (Refs. 29 and 31) and $R_N S = (3\text{--}7) \cdot 10^{-9} \Omega\text{-cm}^2$ for TBJ (Ref. 32), which gave $D = (1\text{--}3) \cdot 10^{-2}$ and $D \approx 10^{-1}$, respectively, with the value of the product of resistivity and mean free path $\rho_{\text{YBCO}}^{\text{YBCO}} l_{\text{YBCO}} = 4 \cdot 10^{-9} \Omega\text{-cm}^2$.

B. Electrophysical properties of bicrystal junctions

The typical CVC of RBJ, presented in Fig. 4, is well described by the resistive model of JJ (Ref. 33). The small value of the excess current (deviation from Ohm’s law) at voltages greater than 10 mV indicates the absence of direct (non-tunneling) conductivity. The dependence of critical current on temperature is close to linear, which is different

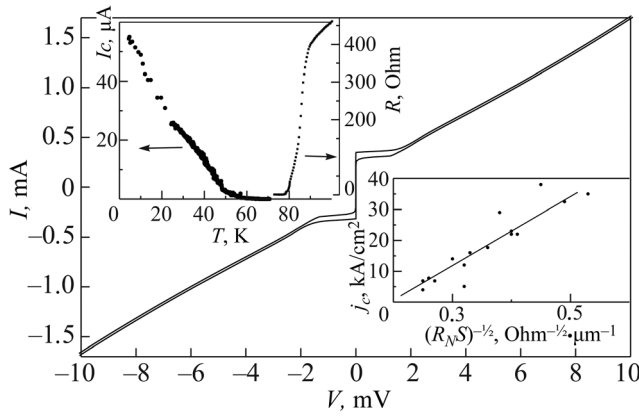


FIG. 4. Current-voltage characteristics of the bicrystal junction at $T = 4.2$ K. The inset on the left shows temperature dependences of the critical current $I_c(T)$ and the resistance of the junction. The inset on the right shows the dependence of the critical current (j_c) density on the characteristic resistance of the boundary $R_N S$.

from the tunnel junctions of S-superconductors,³³ where saturation is observed when $k_B T < \Delta$. In the tunnel DID-transitions, as follows from Fig. 2, both types of states (1) and (2) are observed depending on the angle of incidence of quasiparticles and $I_S(\varphi) = I_{SC}(\varphi) + I_{MGS}(\varphi)$.^{23,34} The contribution of states near the gap (2) increases with temperature according to the Ambegaokar-Baratoff law proportionally to $\Delta^2(T)$,³³ and at low temperature its saturation is $I_{SC} \propto D_0 \Delta_0 \cos 2a \sin \varphi$. At the same time, the contribution of states near the Fermi energy increases with decreasing temperature according to the law $1/T$, and when $k_B T \ll \Delta \sqrt{D}$ it is equal to $I_{MGS} \propto -\Delta_0 \sin 2a \sqrt{D_0} \cos(\varphi/2) \text{ sign}(\sin(\varphi/2))$, with a negative sign. Consequently, there is a characteristic temperature T^* , at which a lapse in the dependence $I_c(T)$ and significant deviation of $I_S(\varphi)$ from sinusoidal dependence should be observed. The estimate of T^* yields a value of about 12 K for transparency $D_0 = 10^{-2}$ for a JJ and $\Delta_0 = 20$ meV for YBCO. In the experiment conducted no lapse in the dependence $I_c(T)$ was observed,³⁰ which may be caused by faceting of the boundary that occurs during the growth of epitaxial films.^{25,26} Note that the lapse in the dependence of $I_c(T)$ was observed in Ref. 23 for an RBJ of small width, comparable to the size of facets. At high temperatures $T_c - T \ll T_c$, at which there is a great influence of thermal fluctuations, the temperature dependence of I_c is close to $(T_c - T)^{1/2}$.^{25,34}

As follows from (1), the superconducting current in the DID-junctions at $T \ll T_c$ is dependent on D ($I_c \propto D^{1/2}$), i.e. different than in SIS junctions, where $I_c \propto D$. This is caused by the fact that E_{MGS} in DID-junctions is near the Fermi energy $E_F \propto \Delta \sqrt{D}$ (see Eq. (1)), and the energy level in SIS-junctions is near the gap $E \propto \Delta$ (Eq. (2)). Indeed, in our experiments the observed dependence is $I_c \propto (R_N S)^{-1/2} \propto D^{1/2}$ (see the inset on the right in Fig. 4). We believe that such a dependence of the energy level on the transparency of the border is resistant to the influence of such factors as boundary faceting, which leads to the formation of both symmetrical $D_x I D_x$ - and asymmetrical $D_x I D_0$ -junctions. However, for $D_x I D_x$ -junctions, as follows from Eq. (1), $I_S \propto \Delta_0 \sqrt{D_0}$ at low temperatures, at the same time for $D_x I D_0$ -junctions $I_S \propto \Delta_0 D_0^2$,^{2,34} therefore when $D < 1$ the superconducting current is defined by areas with a symmetric misorientation of the axes (irregularities in the bicrystal

boundary on a smaller scale (about the Fermi length of quasiparticles $\lambda_F \approx 0.01 \mu\text{m}$) disrupt the coherent Andreev reflection at small angles of incidence of quasiparticle $4\pi\eta\cos\theta/\lambda > \pi$, where η is the degree of boundary inhomogeneity along the direction of current flow⁴¹).

Note that the dependence $I_c \propto D^{1/2}$ was obtained theoretically in SIS-junctions with a wide potential barrier.³⁵ The difference between the energy spectrum of bound states in such SIS-junctions and Eq. (1) causes a different dependence on the barrier transparency. However, for the realization of the mechanism³⁵ necessary are a low barrier transparency $D \leq 10^{-8}$ and a weak influence of depairing factors on the density of states.

Thus, in RBJ formed from CS with a dominant d -type order parameter²⁻⁴ (DID-junctions) both high-energy and low-energy Andreev states are involved in the process of transfer of current.^{30,34,36,37} At the same time, with the characteristic for TBJ orientation of crystallographic axes, when one of the axes of the reference plane of the CS is parallel to the normal to the boundary, the low-energy states do not occur.^{30,34,36,37} The difference between the mechanisms of current flow in the case of RBJ and TBJ also affects the angular dependence of the critical parameters of transitions. Thus, for RBJ it is known that the magnitude of characteristic voltage V_c varies slightly in a large range of misorientation angles up to $\pm 33^\circ$, while normal resistance at the same time can increase by an order of magnitude.³⁸ Note that when $\alpha = \pm 45^\circ$ the current j_c is strongly suppressed, and V_c is reduced by an order of magnitude reaching 0.5 mV at liquid-helium temperature.³⁹ For TBJ the experiment revealed a much stronger angular dependence: with increasing misorientation angle by 6° the parameter V_c decreased by more than three times. Such behavior is in good agreement with theory,⁴⁰ in which taken under consideration are both the ratio of the energy of the superconducting gap to the Fermi energy, $1 > \Delta/E_F > 0$, characteristic for CS, and the significant anisotropy of the Fermi surface. Consideration of these factors leads to the conclusion that in the process of Andreev reflection at the border of the inclined planes quasi-momenta of the incident electron and the reflected hole diverge at a certain angle, the coherence of multiple Andreev reflection is disrupted, and as a result this leads to a decrease of the superconducting current. In this case there must be a certain critical angle of misorientation, at which the critical current drops to zero,⁴⁰ but such a strong dependence can be blurred by the inhomogeneities of the boundary. In RBJ with a small misorientation angle $\alpha + \beta < 13^\circ$ some CVCs are observed that differ from the hyperbolic shape and are typical for the viscous flow of vortices.³³

C. Current-phase relation of superconducting current

The current-phase relation (CPR) of superconducting current of a JJ $I_S(\varphi)$ is determined by the nature of conductivity in the superconducting junction. At high temperatures $T_c - T \ll T_c$ the deviation of the dependence $I_S(\varphi)$ from sinusoidal is small for all types of junctions. At low temperatures $T \ll T_c$ sinusoidal dependence $I_S(\varphi) = I_c \sin \varphi$ is preserved for SIS-junctions regardless of barrier transparency when $D \ll 1$,^{15,33,36} and the SNS-junctions are long (compared to $h v_F / k_B T$) with decreasing temperature. To

determine the deviation of CPR from sinusoidal dependence CVCs were measured under the influence of monochromatic radiation of millimeter range $I_e \sin(2\pi f_e t)$, $f_e = 40\text{--}100\text{ GHz}$.²⁹ We investigated RBJ with symmetrical supply of current, when the bridge is directed perpendicular to the boundary, and junctions with asymmetrical supply of current shift, when the junction bridge is at angle $\gamma = 0\text{--}72^\circ$ to the boundary. Fig. 5 shows the amplitude dependences of the first $I_1(I_e)$ and the subharmonic $I_{1/2}(I_e)$ Shapiro steps for two junctions $\gamma = 0^\circ$ and $\gamma = 54^\circ$. Theoretical CPR, calculated in the resistive model for $f_e > 2eI_c R_N/h$, are presented in the inset in Fig. 5. The calculation was made for a sinusoidal dependence and for the case $I_S(\varphi) = I_{c1}\sin\varphi + I_{c2}\sin 2\varphi$ for $q = I_{c2}/I_{c1} = 0.2$. It is seen that the difference between theoretical and experimental dependences $I_1(I_e)$ is small. A slight deviation of CPR from sinusoidal leads to the appearance of subharmonic Shapiro steps in the CVC of the RBJ. Measurements of the dependence of the amplitude of subharmonic steps on the angle of bridge orientation γ show a lack of the $\sin 2\varphi$ component in the CPR for angles in the range $\gamma = 0\text{--}36^\circ$ with accuracy better than 5%. For angles $\gamma > 40^\circ$ the contribution of current with $\sin 2\varphi$ increases monotonically (for high-frequency external influence $f_e > 2eI_c R_N/h$ in the framework of the resistive model the ratio of the maximum amplitude of the subharmonic step to the critical one is equal to the ratio of the second harmonic to the first in CPR). The reason for the deviation of CPR from sinusoidal in RBJ with large γ is, possibly, the component of current along the bicrystal boundary, which changes the spectrum of low-energy Andreev states. The maximum value of energy of the Andreev states $\Delta_0 \sqrt{D_0} \approx 2\text{ meV}$ is comparable to the energy of the longitudinal component of the superconducting current $\varepsilon = ev_F j_c \lambda_L^2 \approx 5\text{ meV}$ for $j_c = 10^3\text{ A/cm}^2$, $v_F = 5 \cdot 10^4\text{ cm/s}$, and $\lambda_L = 0.1$ is the London penetration depth.

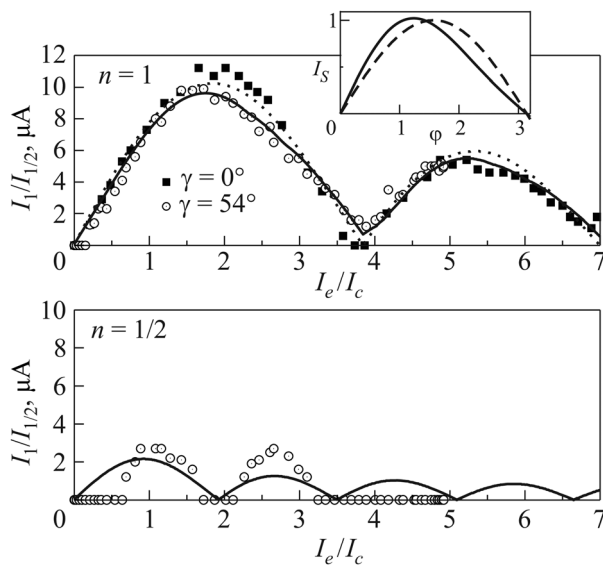


FIG. 5. Dependences of the Shapiro steps (the first $n=1$ and the fractional $n=1/2$) on the amplitude of the external electromagnetic radiation of frequency $f_e = 100\text{ GHz}$ when $T = 4.2\text{ K}$ for two tilt angles of the bridge forming the TBJ. The dotted line represents dependences calculated within the framework of the resistive model for $I_S(\varphi) = I_c \sin\varphi$, the solid line represents $I_S(\varphi) = (1-q)I_c \sin\varphi + qI_c \sin 2\varphi$, $q = 0.2$. The inset shows the corresponding dependences of $I_S(\varphi)$ for $q = 0.2$ (solid line) and $q = 0$ (dotted line).

D. Shot noise in bicrystal junctions

Noise characteristics of JJ were investigated in the autonomous case and in a weak magnetic field ($H < 100\text{ Oe}$), sufficient for suppression of the critical current. Fig. 6 shows the CVC and the dependence of the noise power $P_N(V)$ (noise power was measured in units of temperature due to some peculiarities of calibrating the measuring system) of the JJ in the autonomous case. It can be seen that at high voltages ($V > 30\text{ mV}$) the experimental dependence of $P_N(V)$ coincides with the classical dependence of the shot-noise effective temperature $T_{SH}(V) = (e/2k_B)I(V)R_D$, calculated for the noise spectral density $S_I = 2eI$ for $eV > k_B T$, hf . This condition was satisfied when $V > 0.7\text{ mV}$ for $T = 4.2\text{ K}$ and frequencies $F = 1\text{--}2\text{ GHz}$, at which the measurements were carried out. Previously, dependence of superconducting junctions on the voltage of noise spectral density (similar to that in Fig. 6) was observed in SIS-junctions^{42,43} around voltages above Δ/e . Fig. 6 shows that in a wide range of voltages $0 < V < 30\text{ mV}$ there is an excess of noise T_N over shot-noise $T_{SH}(V)$. At low voltages ($V < 2\text{ mV}$) peaks are observed in $P_N(V)$, caused by the intrinsic Josephson generation at frequencies of HEMP amplifier function. The observed at low voltages sharp change in the differential resistance $R_D(V)$ (not shown in Fig. 6) affects the impedance matching of the sample with the amplifier, therefore below we will discuss spectral density of current noise $S_I(V) \propto 4k_{BTN}/R_D$ and the effective charge $Q(V) = S_I(V)/2I$, which do not depend on R_D . As a result, taking into account changes in $R_D(V)$, for $V > 4\text{ mV}$ an almost linear growth of $S_I(V)$ and a distinct peak in the region where $V < 2\text{ mV}$ were observed. Dependence of $Q(V)$ is shown in the inset in Fig. 6. We see an increase in the effective charge, characteristic for superconducting structures with multiple Andreev reflection.^{5,7,44} The maximum value of Q_{\max} exceeded $10e$ (where e is the charge on the electron).

A significant excess noise intensity caused by the multiple Andreev reflection, above the level of thermal fluctuations, explains the experimentally observed broadening of the Josephson oscillations in CS contacts.^{45,46} In this case we note that at high stresses on the JJ the Nyquist noise is significantly lower than the shot noise.

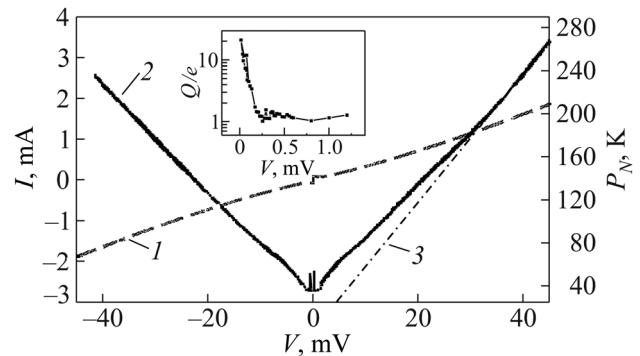


FIG. 6. Current-voltage characteristics for a symmetrical RBJ at $T = 4.2\text{ K}$ (dotted line) and the noise power $P_N(V)$, given in degrees Kelvin (solid line). The dot-dashed line represents the dependence of shot noise $T_{SH}(V) = (e/2k_B)I(V)R_D$. The inset shows the dependence of the effective charge $Q(V) = S_I(V)/2I$ in units of electron charge.

III. HYBRID JOSEPHSON HETEROSTRUCTURES WITH AN ANTIFERROMAGNETIC LAYER

The greatest advances in the study of JJ with a magnetic layer are associated with structures containing ferromagnetic (F) metal layers.^{9,10,47,48} Much less studied are the superconducting structures containing magnetic materials with antiferromagnetic (AF) ordering. Such materials are of particular interest due to the possibility of managing their properties (and hence the parameters of weak coupling) due to the influence of weak external magnetic field. This circumstance was first addressed by L. Gorkov and V. Kresin,⁴⁹ who theoretically analyzed the critical current of superconducting structures with an AF-layer and predicted a strong dependence of the critical current on magnetic field. The first experimental data on the Josephson current flow in an S–AF–S structure were obtained in junctions based on Nb with an FeMn layer,⁵⁰ however, no anomalous behavior was discovered in magnetic field dependences on the critical current.

Giant proximity effect was often observed in the CS with a cuprate barrier layer, found in the antiferromagnetic state;^{11,14} possible interpretation of the observed in Ref. 14 effect was proposed in Ref. 51. In this section presented are the results of an experimental study of the magnetic-field characteristics of superconducting current in hybrid mesaheterostructures Nb/Au/Ca_{1-x}Sr_xCuO₂/YBa₂Cu₃O_{7-δ} based on epitaxial films of CS YBa₂Cu₃O_{7-δ} (YBCO) and niobium (Nb), where Au represents gold film used to diminish oxygen diffusion from YBCO, and the Ca_{1-x}Sr_xCuO₂ (CSCO) layer at low temperatures is a quasi-two-dimensional Heisenberg antiferromagnetic with Neel temperature of over 500 K.^{52,53}

A. Experimental method

Epitaxial heterostructures CSCO/YBCO were deposited on substrates of NdGaO₃ by laser ablation at $T = 800^\circ\text{C}$. After cooling, the Au film was deposited without breaking the vacuum. CSCO was made with either $x = 0.15$ or $x = 0.5$. The thickness of the AF-layer was varied in $d_M = 20\text{--}50\text{ nm}$. The layer of Nb and the additional layer of Au were deposited by magnetic sputtering. The topology of hybrid mesaheterostructure (HMS) was formed by photolithography, and by plasma-chemical and ion-beam etching.^{12,13,54} Cross-section of the HMS is shown in Fig. 7(a), and the shape of HMS is a square of linear size $L = 10\text{--}50\ \mu\text{m}$, included in the log-periodic antenna applied for the measurement in an electromagnetic field in the millimeter wavelength range (see Fig. 7(b)). For the measurement of electrophysical characteristic

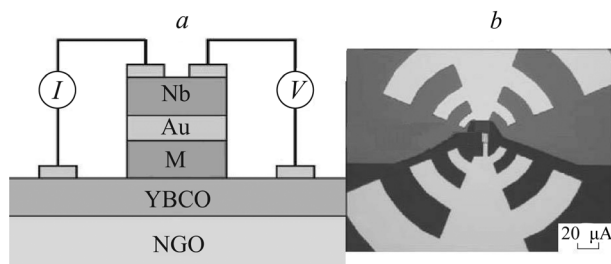


FIG. 7. (a) Cross section of the heterostructure with an AF (CSCO) interlayer, marked with the letter M. The thicknesses of the layers: YBCO–200 nm, CSCO–20–50 nm, Au–10–20 nm, Nb–200 nm. (b) A photograph of HMS from the top. The light color represents superconducting electrodes of the log-periodic antenna.

of the HMS a contact was connected to the upper Nb electrode and two—to the YBCO film (Fig. 7(a)). In this case for $T < T_c$ (where T_c is the critical temperature of the YBCO-film) the resistance measurements of CSCO layer and the Au/CSCO interface were conducted by four-point scheme. According to preliminary measurements, the resistance of Au, Nb, and CSCO films and the CSCO/YBCO interface can be neglected.^{12,13} As a result, the obtained structures with an AF-layer can be regarded as S–N–I_b–AF–D-junctions, where the role of the barrier I_b is fulfilled by the Au/CSCO boundary. For comparison, HMS Nb/Au/YBCO without the AF interlayer were prepared and studied. Measurements of both types of structures were carried out under the same conditions.

B. The superconducting current in HMS

Dependences of the critical current of the entire HMS on the temperature $I_c(T)$ as a whole follow the temperature dependence of the superconducting parameter Δ_{Nb} in the Nb film – similarly to structures without and AF-interlayer.⁵⁴ As in all the investigated HMS with an AF-interlayer thickness d_M is around tens of nanometers, the penetration depth of the superconducting order parameter in CSCO significantly exceeds that observed in Ref. 50 for a polycrystalline layer of FeMn.

Estimates of the penetration depth of superconducting correlations in CSCO can be made on the basis of measurements of the dependence of superconducting current density on thickness $j_c(d_M)$. Fig. 8 shows the experimental data and theoretical dependences (dotted line) $j_c(d_M)$ for three values of normalized exchange field $H_{\text{ex}}/\pi k_B T$ in F-layers of the S'/I/M/S-structure with an AF-layer (modeled $N = 20$ —the number of F-layers of oppositely directed magnetization), obtained for $\xi_{\text{AF}} = 10\text{ nm}$.⁵⁵ Theoretical dependences are shown for the case of low transparency of the M/S–boundary (greater than I-barrier transparency) and identical superconductors S and S'. Note that qualitatively the shape of theoretical dependences $j_c(d_M)$ does not change even in

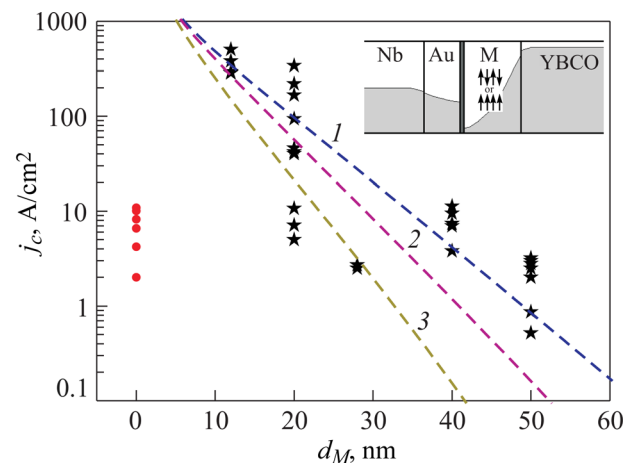


FIG. 8. Experimental data on the dependence of the density of superconducting current on the thickness for an HMS with an interlayer of CSCO (stars) $x = 0.5$. Filled circles correspond to heterotransitions without the M-interlayer. The dashed lines show the theoretical dependences of critical current on the thickness of the AF-interlayer for three values of normalized exchange field $H_{\text{ex}}/\pi k_B T$: 2 (1), 5 (2), 10 (3). The normalization of the theoretical dependence in the critical current value and the interlayer thickness was chosen from the condition of best fit to the theory of experiment $\xi_{\text{AF}} = 10\text{ nm}$.

the case of unequal superconductors. In our experiment the superconductors are different; moreover, in YBCO the condensate function with s -symmetry is not primary. However, for normalized values of $j_c(d_M)$, presented in Fig. 8, the condensate Green's function of electrodes does not play a principal role. Statistical analysis of the dependence $j_c(d_M)$ gives the depth of decay of the superconducting wave function $\xi_{AF} = (7 \pm 1)$ nm. It is seen that the theoretical dependence $j_c(d_M)$ for $H_{ex}/\pi k_B T = 2$ better describes the experimental data, then the dependences obtained for large values of $H_{ex}/\pi k_B T$. Recall, a radical contrast of the Josephson current in S/AF/S-junctions for the cases of even and odd numbers of layers N was predicted earlier in the works, which analyzed a model of an antiferromagnetic with atomic-thin layers (e.g. see Ref. 56). The case of structures containing an arbitrary number of ferromagnetic layers (significantly exceeding the atomic size) with antiferromagnetic ordering of magnetization, in particular, the dependence of transport properties on the number of layers, has been studied in Ref. 57.

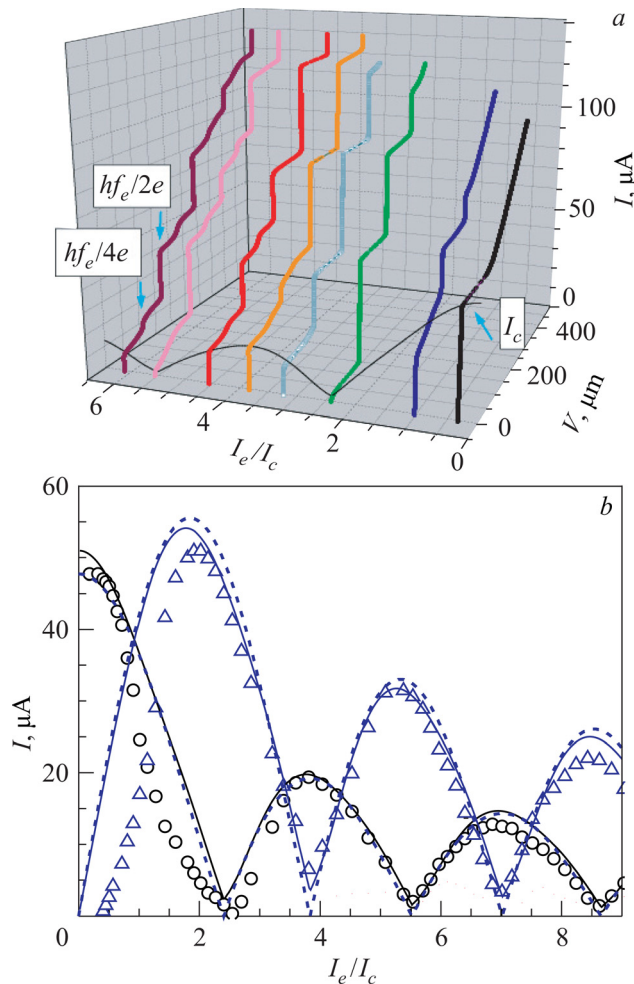


FIG. 9. (a) The family of CVC HMS at various values of the power of microwave impact and $T = 4.2$ K. The thin line shows the envelope of the critical current, arrows show the first ($hf_e/2e$) and fractional ($hf_e/4e$) Shapiro steps. (b) The dependence of critical current I_c (circles) and the first Shapiro step I_1 (triangles) on the normalized amplitude I_e/I_c of external influence of millimeter radiation with frequency of 56 GHz for $T = 4.2$ K. The dashed line shows the theoretical dependence $I_1(I_e/I_c)$, obtained from the resistive model of JJ. The solid line shows the calculated dependences calculated with the second CPR harmonic in mind for $q = 0.2$.

C. The current-phase relation

Autonomous man CVC HMS (see Fig. 9(a)) around low voltages ($V \leq 1$ mV) is nearly hyperbolic, typical for a JJ. In the voltage range $V \geq 5$ mV for temperatures $T_c > T > T'_c$ (where T'_c is the temperature of Nb film) conductivity anomalously with a maximum at $V = 0$ was observed, caused, most likely, by the Andreev states of low energy.^{13,55} When $T < T'_c$ characteristics were observed in the dependence of the differential resistance of the HMS on voltage $R_D(V)$, which were due to the superconducting gap in niobium. It is known^{48,58} that the mixed (d - and s -) symmetry of the order parameter of one of the electrodes if the JJ contributes to the second harmonic in the current-phase relationship (CPR). For the determination of the deviation of CPR from sinusoidal dependence we used a previously developed method based on measuring the amplitudes of Shapiro steps, resulting from synchronizing the intrinsic Josephson generation by external monochromatic microwave signal at frequency f_e (Ref. 58) (see Fig. 9(a)). Oscillatory dependences of the critical current and the first Shapiro step on the normalized amplitude of external effect I_e/I_c (Fig. 9(b)) confirm the Josephson nature of the superconducting current. There is a satisfactory agreement between the critical frequency $f_c = 2eV_c/h = 50$ GHz, determined from the maximum value of the first Shapiro step in the resistive model (see the dotted line in Fig. 9(b)) with $f_c = 70$ GHz, obtained from the measured under dc value $V_c = 145 \mu\text{m}$, which indicates the uniformity of current flow in the structure and the absence of short-circuiting. The best match of the maximum value of the first Shapiro step and the calculations is observed taking into account the second harmonic $\sin 2\varphi$ in the CPR. In contrast to bicrystal junctions, HMS have more capacity, which strongly affects the dynamic parameters of JJ, in particular, causes the appearance of fractional Shapiro steps. According to the calculations in the framework of a modified resistive model,⁵⁹ taking into account the capacity of HMS and the presence of I_{c2} (solid line in Fig. 9(b)), the ratio of the amplitude of the second harmonic to the first for the structure, presented in Fig. 9(b), is $q = I_{c2}/I_{c1} = 0.2$.

The deviation of CPR from sinusoidal relation is also confirmed by measurements of the amplitudes of the primary η_1 and the subharmonic $\eta_{1/2}$ detector response, carried out in a weak electromagnetic field with power P on the order of a few pW, which excluded the possibility of the appearance of fractional Shapiro steps as a result of external pumping. The thus obtained weight estimates of the second CPR harmonic according to the formula $|q| \approx 0.5(\max \eta_{1/2}/\max \eta_1)^{1/2}$ (Refs. 57 and 58) gave values close to those obtained in the analysis of the oscillatory dependences of Shapiro steps.

D. Magnetic-field dependence

As shown theoretically,⁴⁹ in an S-AF-S-structure with an interlayer of a layered A-type antiferromagnet (see inset in Fig. 10(a)) there is a critical current I_c , which is dependent on the external magnetic field H , causing the changes in the parameters of the AF-layer,

$$I_c(H) \approx I_c^0 \left(\frac{2}{\pi \beta M_S} \right)^{1/2} \left| \cos \left(\beta M_S - \frac{\pi}{4} \right) \right|, \quad (3)$$

where $\beta \gg 1$ characterizes the electronic structure of the AF-interlayer; $0 < M_S < 1$ is the parameter of

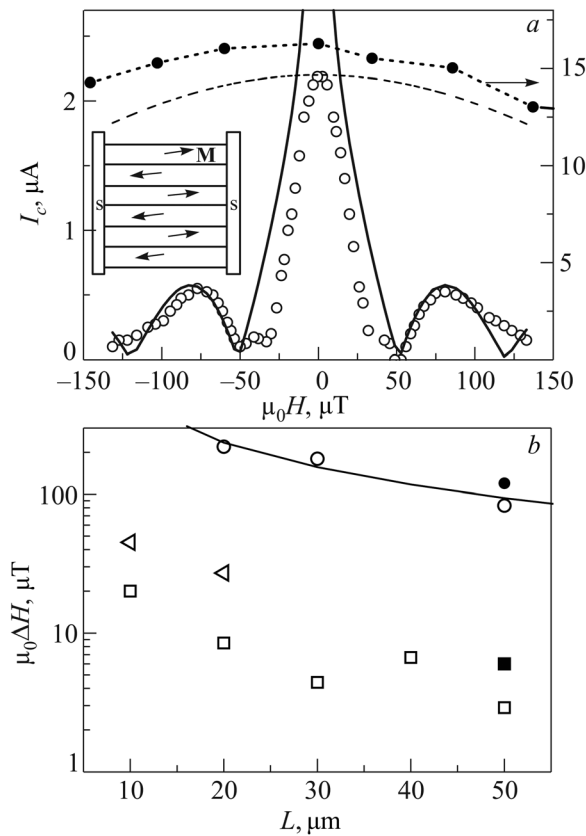


FIG. 10. (a) The magnetic field dependence of the critical current $I_c(H)$ (circles) for a HMS containing CSCO ($x=0.5$), $d_M=50$ nm, and $L=10$ μm at $T=4.2$ K. The solid line represents the dependence of Eq. (3) under the normalization $I_c(0)=I_c^0$. Dashed line shows calculated Fraunhofer dependence for $L=10$ μm and London penetration depths $\lambda_{L1}=150$ nm and $\lambda_{L2}=90$ nm for YBCO and Nb, respectively. Filled circles – experimental data for a heterostructure without AF-interlayer with $L=50$ μm . Inset: model⁵⁰ for an S–AF–S JJ. (b) Dependence of the first minimum H_1 on the magnitude of HMS: without an AF-interlayer for a perpendicularly directed field (\circ), for the parallel field (\bullet); HMS with $d_M=50$ nm for a perpendicular field (\square), for a parallel field (\blacksquare), $d_M=20$ nm (\triangle); solid line—approximation of the $1/L$ type.

antiferromagnetic ordering, dependent on the spatial components of local magnetization of F-layers and the external magnetic field H ; I_c^0 is the critical current in the absence of an external field, the magnitude of which coincides with the value of I_c in the equivalent S–N–S structure.⁴⁹ In Ref. 49 I was also shown that the decay of the superconducting order parameter in the AF-interlayer is determined by its metallic conductivity and in the clean limit it equals $\xi_{AF} = \hbar v_F / k_B T$, where v_F is the Fermi velocity in the interlayer.

From Eq. (3) it follows that the period of dependence of $I_c(H)$ for the S–AF–S-structure differs significantly from the “Fraunhofer” dependence period, typical for JJs with a homogeneous barrier layer.⁵⁹ The Fraunhofer dependence zeros correspond to the inclusion in the JJ of a whole number of magnetic flux quanta $\Phi_0 = h/2e = 2.07 \cdot 10^{-15}$ Wb. According to (3), the zeros of $I_c(H)$ correspond to the condition $\beta M_S = \pi/4 + \pi n$ ($n=1,2,\dots$). And, when $\beta \gg 1$ oscillations of $I_c(H)$ can be observed in small magnetic fields.⁴⁹

Fig. 10(a) shows the dependence $I_c(H)$ for a structure with an AF layer of thickness $d_M=50$ nm of CSCO-film with $x=0.5$ and $L=10$ μm . For comparison, Fig. 10(a) shows the dependence $I_c(H)$ for a heterostructure without an AF layer. It can be seen that for an HMS with an AF-layer the magnitude

of H_1 is significantly smaller than the field of the first minimum for the structure without an interlayer. Considering that the measurements were carried out under the same experimental conditions and on samples with identical geometry, the decrease of the external magnetic field H_1 by more than an order magnitude, necessary to obtain the first minimum $I_c(H)$ in structures with an CSCO-layer compared to the structures without an interlayer, can be associated with the presence of an AF-interlayer. A solid line represents the dependence of Eq. (3) with experimental parameters I_c^0 and the first minimum of H_1 for the power indicator corresponding to coefficient $[(\pi/2)\beta M_S]$ in (3), equal to -0.75 —not -0.5 , as in the theory presented in Ref. 49. The deviation of the experimental points from the solid line in Fig. 10 at low H is due to the limitations of applying equation (3) for M_S close to zero.⁴⁹ Based on the widened secondary maxima, the periodicity of the shape of $I_c(H)$ structures with an AF-interlayer (Fig. 10(a)) is closer to Eq. (3) with $H_1 \approx 1/2 (H_2 - H_1)$, while in a Fraunhofer dependence $H_1 \approx H_2 - H_1$.

Fig. 10(b) shows the dependence of H_1 on the magnitude of HMS for both the structures with and without an AF interlayer. A significant decrease in the magnitude of H_1 upon adding an AF-interlayer is not explained by the increase in London penetration depth λ_{L1} of YBCO because of the decrease in the level of oxygen doping of the YBCO-film adjacent to the barrier layer Au/CSCO (no more than 30% for the critical temperature of YBCO—40 K).⁶⁰ According to Ref. 49, nonmonotonic dependence $I_c(H)$ with periodicity, which is different than the magnetic flux quantum in S–AF–S-junctions, is caused by a small change in the tilt of magnetic moments in ferromagnetic layers under the influence of an external magnetic field and, therefore, the M_S parameter in Eq. (3) (see the inset in Fig. 10(a)). As a result, the $I_c(H)$ minima are observed at significantly lower values of the external magnetic field, than the value of $H_1 = \Phi_0 / \mu_0 d_e L$, which corresponds to the penetration of the magnetic flux quantum Φ_0 into the structure.

IV. CONCLUSION

Experimental investigation of the dependences of the critical current on the temperature, barrier transparency, and phase difference of superconducting electrodes, as well as the shape of CVC, showed that the most likely mechanism of superconducting current flow in the main plane of bicrystal junctions in cuprate superconductors is the transfer of charge through the barrier involving bound states at the superconductor–insulator boundary, appearing as a result of multiple Andreev reflection. However, the shapes of current-phase and magnetic field dependences of the critical current cannot be described within the framework of the homogeneous transition model without taking into consideration the boundary roughness, which is due to boundary faceting, arising with the growth of epitaxial films. At the present time there is not a complete theory which corresponds to the experimental situation. Around high bias voltages ($V > 5$ mV) excess transition noise was discovered above thermal fluctuations, coinciding with the dependence on voltage at the shot-noise transition, exactly as in superconducting tunneling junctions made of S-superconductors. Near low voltages a noise peak is observed, which is characteristic for

superconducting junctions, in which there is multiple Andreev reflection.

In oxide hybrid mesa-structures with antiferromagnetic interlayer the superconducting current, which is Josephson in nature, was measured experimentally. We discovered deviation in the current-phase dependence of superconducting current from sinusoidal dependence as a result of 20% contribution of the second harmonic ($\sim \sin 2\varphi$). Unlike in known Josephson structures, in the hybrid mesa-structures there is a critical current modulation, caused by the influence of external magnetic field on the magnetization vector of the antiferromagnetic interlayer. As a result, sensitivity to external magnetic field increases almost by an order of magnitude.

We thank I. V. Borisenko, D. Winkler, V. V. Demidov, A. V. Zaitsev, Yu. V. Kislinsky, A. Kalabukhov, F. V. Komissinsky, V. K. Kornev, E. Myugind, A. M. Petrzhik, I. I. Soloviev, A. V. Shadrin for the help in conducting the experiment and the useful discussion. The study was supported through the OFN RAS and the RAS Presidium programs, by the Ministry of Education and Science of Russia (Grant 02.740.11.0795), the Russian Presidential grant: Leading Scientific School (Grant NSh-2453.2012.2), by the project RFFI-11-02-01234 a, and Visby—the program of Russian-Swedish cooperation.

^{a)}Email: gena@hitech.cplire.ru

- ¹E. E. Il'ichev, M. Grajcar, R. Hlubina, A. Marx, S. Kleefisch, T. Bauch, H. Sato, M. Naito, and G. Koren, *Phys. Rev. Lett.* **86**, 5369 (2001).
- ²L. Alff, A. Beck, R. Gross, I. V. Borisenko, and K. Y. Constantinian, *Phys. Rev. B* **58**, 11197 (1998).
- ³G. A. Ovsyannikov, A. D. Mashtakov, I. V. Borisenko, and K. Y. Constantinian, *J. Low Temp. Phys.* **117**, 605 (1999).
- ⁴A. D. Mashtakov, K. I. Konstantinian, G. A. Ovsyannikov, and E. A. Stepantsov, *Pis'ma Zh. Tekh. Fiz.* **25**, 1 (1999).
- ⁵E. V. Bezuglyi, E. N. Bratus', V. S. Shumeiko, and G. Wendin, *Phys. Rev. Lett.* **83**, 2050 (1999).
- ⁶Y. Naveh and D. V. Averin, *Phys. Rev. Lett.* **82**, 4090 (1999).
- ⁷K. Y. Constantinian, G. A. Ovsyannikov, I. V. Borisenko, J. Mygind, and N. F. Pedersen, *IEEE Trans. Appl. Supercond.* **13**, 610 (2003).
- ⁸J. C. Cuevas and M. Fogelström, *Phys. Rev. B* **64**, 104502 (2001); *Phys. Rev. Lett.* **89**, 227003 (2002).
- ⁹A. I. Buzdin, *Rev. Mod. Phys.* **77**, 935 (2005).
- ¹⁰F. S. Bergeret, A. F. Volkov, and K. B. Efetov, *Rev. Mod. Phys.* **77**, 1321 (2006).
- ¹¹I. Bozovic, G. Logvenov, M. A. J. Verhoeven, P. Caputo, E. Goldobin, M. R. Beasley, and T. H. Geballe, *Phys. Rev. Lett.* **93**, 157002 (2004).
- ¹²G. A. Ovsyannikov, I. V. Borisenko, F. V. Komissinsky, Yu. V. Kislinsky, and A. V. Zaitsev, *Pis'ma Zh. Eksp. Teor. Fiz.* **84**, 320 (2006).
- ¹³P. Komissinskiy, G. A. Ovsyannikov, I. V. Borisenko, Yu. V. Kislinskii, K. Y. Constantinian, A. V. Zaitsev, and D. Winkler, *Phys. Rev. Lett.* **99**, 017004 (2007).
- ¹⁴Y. Tarutani, T. Fukazawa, U. Kabasawa, A. Tsukamoto, Mo Hiratani, and K. Takagi, *Appl. Phys. Lett.* **58**, 2707 (1991).
- ¹⁵I. O. Kulik and I. K. Yanson, *Josephson Effect in Superconducting Tunneling Structures* (Nauka, Moscow, 1970).
- ¹⁶I. O. Kulik, *Zh. Eksp. Teor. Fiz.* **30**, 944 (1970).
- ¹⁷A. Furusaki and M. Tsukada, *Phys. Rev. B* **43**, 10164 (1991).
- ¹⁸C.-R. Hu, *Phys. Rev. Lett.* **72**, 1526 (1994).
- ¹⁹M. Covington, M. Aprili, E. Paraoanu, L. H. Greene, F. Xu, J. Zhu, and C. A. Mirkin, *Phys. Rev. Lett.* **79**, 277 (1997).
- ²⁰F. V. Komissinsky, G. A. Ovsyannikov, Yu. V. Kislinsky, I. M. Kotelyansky, and Z. G. Ivanov, *Zh. Eksp. Teor. Fiz.* **122**, 1247 (2002).
- ²¹Yu. S. Barash, *Phys. Rev. B* **61**, 678 (2000).
- ²²C. W. J. Beenakker, *Phys. Rev. Lett.* **67**, 3836 (1991).
- ²³E. Il'ichev, V. Zakosarenko, R. P. Ijsselsteijn, V. Schultze, H. G. Meyer, H. E. Hoinig, H. Hilgenkamp, and J. Mannhart, *Phys. Rev. Lett.* **81**, 894 (1998).
- ²⁴T. Lofwander, V. S. Shumeiko, and G. Wendin, *Supercond. Sci. Technol.* **14**, R53 (2001).
- ²⁵H. Hilgenkamp and J. Mannhart, *Rev. Mod. Phys.* **74**, 485 (2002).
- ²⁶D. Dimos, P. Chaudhari, and J. Mannhart, *Phys. Rev. B* **41**, 4038 (1990).
- ²⁷A. D. Mashtakov, G. A. Ovsyannikov, I. V. Borisenko, I. M. Kotelyanskii, K. Y. Constantinian, Z. G. Ivanov, and D. Ertz, *IEEE Trans. Appl. Supercond.* **9**, 3001 (1999).
- ²⁸I. K. Bdikin, A. D. Mashtakov, P. B. Mozhaev, and G. A. Ovsyannikov, *Physica C* **334**, 168 (2000).
- ²⁹G. A. Ovsyannikov, I. V. Borisenko, and K. Y. Constantinian, *Vacuum* **58**, 149 (2000).
- ³⁰I. V. Borisenko, K. I. Constantinian, Yu. V. Kislinsky, and G. A. Ovsyannikov, *Zh. Eksp. Teor. Fiz.* **126**, 1402 (2004).
- ³¹G. A. Ovsyannikov, I. V. Borisenko, K. I. Constantinian, A. D. Mashtakov, and Ye. A. Stepantsov, *Pis'ma Zh. Eksp. Teor. Fiz.* **25**, 65 (1999).
- ³²I. V. Borisenko, A. V. Shadrin, G. A. Ovsyannikov, I. M. Kotelyanskii, F. B. Shadrin, G. A. Ovsyannikov, I. M. Kotelyanskii, and F. V. Komissinsky, *Pis'ma Zh. Eksp. Teor. Fiz.* **31**, 22 (2005).
- ³³K. K. Likharev, *Rev. Mod. Phys.* **51**, 102 (1979).
- ³⁴Yu. S. Barash, A. A. Svidzinsky, and H. Burkhardt, *Phys. Rev. B* **55**, 15282 (1997).
- ³⁵G. Wendin and V. S. Shumeiko, *Phys. Rev. B* **53**, R6006 (1996).
- ³⁶R. A. Riedel and P. F. Bagwell, *Phys. Rev. B* **57**, 6084 (1998).
- ³⁷Y. Tanaka and S. Kashiwaya, *Phys. Rev. B* **53**, R11957 (1996).
- ³⁸U. Pope, Y. Y. Divin, M. I. Faley, J. S. Wu, C. L. Jia, P. Shadrin, and K. Urban, *IEEE Trans. Appl. Supercond.* **11**, 3768 (2001).
- ³⁹F. Tafuri, F. Carillo, F. Lombardi, F. Mileto Granozio, U. Scotti di Uccio, G. Testa, E. Sarnelli, K. Verbit, and G. Van Tendeloo, *Supercond. Sci. Technol.* **12**, 1007 (1999).
- ⁴⁰A. Golubov and F. Tafuri, *Phys. Rev. B* **62**, 15200 (2000).
- ⁴¹M. B. Walker and P. Pairor, *Physica C* **341–348**, 1523 (2000).
- ⁴²P. L. Richards, T. M. Shen, R. E. Harris, and F. L. Lloyd, *Appl. Phys. Lett.* **36**, 480 (1980).
- ⁴³Y. Blanter and M. Buttiker, *Phys. Rep.* **336**, 1 (2000).
- ⁴⁴Y. Naveh and D. V. Averin, *Phys. Rev. Lett.* **82**, 4090 (1999).
- ⁴⁵K. Y. Constantinian, G. A. Ovsyannikov, I. V. Borisenko, N. G. Pogosyan, A. A. Hakhoumian, P. Yagoubov, J. Mygind, and N. F. Pedersen, *Supercond. Sci. Technol.* **14**, 1035 (2001).
- ⁴⁶Y. Y. Divin, U. Pope, K. Urban, O. Y. Volkov, V. V. Shiroto, V. V. Pavlovskii, P. Schmueser, K. Hanke, M. Geitz, and M. Tonutti, *IEEE Trans. Appl. Supercond.* **9**, 3346 (1999).
- ⁴⁷A. A. Golubov, M. Yu. Kupriyanov, and E. Il'ichev, *Rev. Mod. Phys.* **76**, 411 (2004).
- ⁴⁸V. Ryazanov, V. A. Oboznov, A. Yu. Rusanov, A. V. Veretennikov, A. A. Golubov, and J. Aarts, *Phys. Rev. Lett.* **86**, 2427 (2001); *J. Low Temp. Phys.* **136**, 385 (2004).
- ⁴⁹L. P. Gorkov and V. Z. Kresin, *Physica C* **367**, 103 (2002).
- ⁵⁰C. Bell, E. J. Tarte, G. Burnell, C. W. Leung, D.-J. Kang, and M. G. Blamire, *Phys. Rev. B* **68**, 144517 (2003).
- ⁵¹K.-U. Barholtz, M. Yu. Kupriyanov, U. Hübner, F. Schmidl, and P. Seidel, *Physica C* **334**, 175 (2000).
- ⁵²D. Vuknin, E. Caignol, P. K. Davis, J. E. Fischer, D. C. Johnston, and D. P. Goshorn, *Phys. Rev. B* **39**, 9122 (1989).
- ⁵³G. A. Ovsyannikov, S. A. Denisyuk, and I. K. Bdikin, *Fiz. Tverd. Tela* **47**, 417 (2005).
- ⁵⁴Yu. V. Kislinsky, F. V. Komissinsky, K. I. Constantinian, G. A. Ovsyannikov, T. Yu. Karniskaya, I. I. Soloviev, and V. K. Kornev, *Zh. Eksp. Teor. Fiz.* **128**, 575 (2005).
- ⁵⁵G. A. Ovsyannikov, K. Y. Constantinian, Yu. V. Kislinski, A. V. Shadrin, A. V. Zaitsev, A. M. Petrzhik, V. V. Demidov, I. V. Borisenko, A. V. Kalabukhov, and D. Winkler, *Supercond. Sci. Technol.* **24**, 055012 (2011).
- ⁵⁶B. M. Andersen, I. V. Bobkova, P. J. Hirschfeld, and Yu. S. Barash, *Phys. Rev. Lett.* **96**, 117005 (2006).
- ⁵⁷A. V. Zaitsev, *Pis'ma Zh. Eksp. Teor. Fiz.* **83**, 277 (2006).
- ⁵⁸P. V. Komissinskiy, G. A. Ovsyannikov, K. Y. Constantinian, Y. V. Kislinskii, I. V. Borisenko, I. I. Soloviev, V. K. Kornev, E. Goldobin, and D. Winkler, *Phys. Rev. B* **78**, 024501-15 (2008).
- ⁵⁹A. Barone and J. Paterno, *The Josephson Effect. Physics and Applications* (Mir, Moscow, 1984).
- ⁶⁰M. R. Trunin, *Usp. Fiz. Nauk* **175**, 1017 (2005).

Translated by D. K. Maraoulaite